Surface Initiation from Adsorbed Polymer Clusters: A Rapid Route to Superhydrophobic Coatings

Juan C. Tuberquia and G. Kane Jennings*

Department of Chemical and Biomolecular Engineering, Vanderbilt University, Nashville, Tennessee 37235, United States

S *Supporting Information*

ABSTRACT: We introduce the use of a hydroborated polyisoprene (PIP) macroinitiator for the rapid surface-initiated growth of superhydrophobic polymethylene (PM) films. Rinsing of a dip-coated PIP film on a methyl-terminated surface atop silicon or gold substrates results in robustly bound, isolated PIP clusters. After hydroboration of the internal olefins, these clusters result in extremely rapid growth of polymethylene coatings upon exposure to a diazomethane solution in diethyl ether at -17 °C. The resulting PM films achieve 6 μm thicknesses within 20 min of polymerization and become superhydrophobic with advancing and receding water contact angles of 166° and 156°, respectively, within 1 min. The PM films grown from these PIP clusters exhibit 3× greater propagation velocities, 30% lower termination rates, and more highly textured morphologies than PM films grown from hydroborated monolayers.

KEYWORDS: *superhydrophobic, polymethylene, macroinitiator, surface-initiated, kinetics, topography, borane*
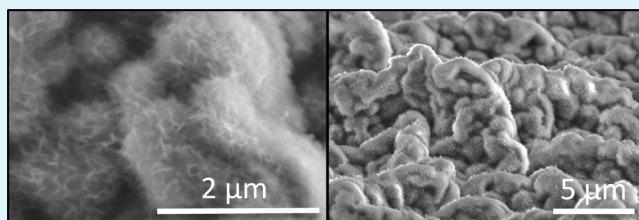
INTRODUCTION

Imparting the requisite microscale roughness to a low-energy surface can yield superhydrophobic (SH) properties[1,2] where an aqueous liquid only contacts the surface at peaks of rough features, entrapping air between the solid and liquid interfaces, as revealed by a variety of techniques.[3,4] This air interlayer provides the most attractive characteristic for multiple applications,[5-8] including corrosion resistance, interfacial slip, and self-cleaning surfaces. As a result of the intense research and great potential of these surfaces, a variety of creative methodologies has been developed to prepare interfaces with SH properties.[2] Nonetheless, many of these approaches would be challenged to transcend the lab scale due to high costs for materials and/or processing. In contrast, some recent wet etch-based approaches are extremely rapid and inexpensive[9,10] but are specific to certain substrates. New strategies are needed to rapidly[11,12] extend superhydrophobicity to a wide variety of substrates with inexpensive, straightforward processing.

Here, we introduce a rapid surface-initiated process to achieve SH coatings on initially smooth surfaces from the world's simplest and most common polymer, polymethylene (PM) (or the chemically equivalent polyethylene). This approach uses straightforward wet processing with excellent control over film thickness and can be easily extended to larger surface areas. Specifically, this study shows that SH PM films can be grown by the polymethylenation of diazomethane from borane initiation sites immobilized on adsorbed polyisoprene (PIP) clusters (Scheme 1). First, we coat a methyl-terminated surface with clusters of PIP as an olefin-rich polymer. To activate the PIP, we hydroborate the olefin moieties with a solution of borane (BH$_3$) in tetrahydrofuran (THF) under inert

Scheme 1. Process for Growing Superhydrophobic PM Films from Hydroborated PIP Clusters
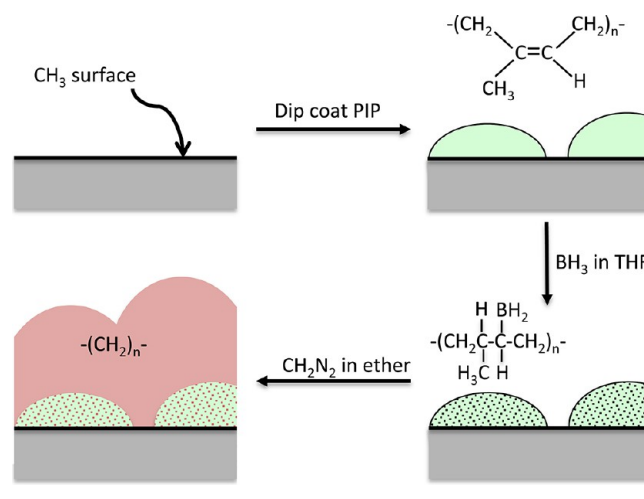
atmosphere. Polymethylenation is accomplished by exposing the surface to a dilute solution of diazomethane (DM) in diethyl ether for as little as 1 min to produce SH polymethylene (PM) films. We specifically chose PIP because its olefin character allows it to be used as an initiation layer, once modified by borane, and its adhesive properties favor its stability upon functionalization. The PIP adheres well to low-

energy methyl-surfaces, which can be prepared on a wide variety of initial substrates through self-assembly. We envision that other elastomers beyond PIP could be used as well, such as neoprene and polybutadiene. Use of polymers as the olefin-containing material provides a key advantage in terms of the high number of olefin groups per chain (each repetitive unit has a moiety susceptible to be functionalized and become an initiator) in comparison to vinyl-terminated monolayers where the initiators would be limited as a 2-D sheet at the interface. Further, the formation of microscale clusters by these olefin-containing polymers when dip coated could increase the roughness of the surface-grown coating. The significance of these aspects allows the rapid growth of sufficiently thick films with greater roughness as compared to films grown from conventional 2-D functional surfaces.

This platform uses the fundamentals of the surface-initiated polymethylenation (SIPM)[13] chemistry recently developed in our group to grow SH films, where vinyl-terminated assembled monolayers have typically served as the initial layer that undergoes hydroboration and subsequent polymerization. In that approach, 24 h of polymethylenation are typically required to achieve sufficient thickness and roughness to produce superhydrophobicity. However, in the present work, we activate an olefin-rich polymer deposited on a low-energy surface, which can propagate the growth of a SH PM film with unique morphology in times that are orders of magnitude faster.

■ EXPERIMENTAL SECTION

Materials. Ethanol (ACS/USP grade) and *n*-octadecyltrichlorosilane were purchased from AAPER and United Chemical Technologies, respectively, and used as received. Hexane (HPLC grade) and concentrated sulfuric acid (95−98%) were used as received from EMD Chemicals. Benzoic acid (ACS grade), toluene (ACS grade), and hydrogen peroxide (30%, ACS grade) were used as received from Fisher Scientific. Nitrogen was obtained from J&M Cylinder Gas, Inc. 1-Octadecanethiol, borane-tetrahydrofuran (THF) complex solution (1.0 M), anhydrous diethyl ether (>99%), *cis*-polyisoprene (M_w ~38 000 by GPC, made from natural rubber), and anhydrous tetrahydrofuran (>99.9%) were acquired from Sigma-Aldrich. Undec-10-ene-1-thiol was synthesized as reported in our previous work.[13] Deionized water (16.7 MΩ·cm) was purified using a Modu-Pure system and used for rinsing. Gold shot (99.99%) and chromium-coated tungsten filaments were purchased from J&J Materials and R. D. Mathis, respectively. Silicon wafers (100) were obtained from Montco Silicon, rinsed with water and ethanol, and dried in a stream of nitrogen.

Preparation of Diazomethane (DM). DM was carefully synthesized according to literature to produce a 16 mM solution in diethyl ether.[14] According to each experiment, the original DM solution was diluted in diethyl ether to the targeted concentration and stored at −17 °C. The concentration of DM was determined by titration with benzoic acid.[14] *Caution:* Diazomethane is toxic and potentially explosive and should be handled carefully.[14]

Preparation of Gold Substrates. Gold substrates were used to perform the IR characterization of each modification step. For this purpose, silicon (100) wafers were rinsed with water and ethanol and dried in a stream of N_2 prior to placement in a metal atom evaporator and reducing the pressure to 4×10^{-6} Torr with a diffusion pump. Then, chromium (100 Å) and gold (1250 Å) were evaporated in sequence onto silicon at rates of 1−2 Å s^{-1}. After bringing the chamber to atmospheric pressure and removing the gold-coated silicon wafers, 1.2 cm × 4 cm gold samples were cut from the wafer, rinsed with ethanol, and dried with N_2 before use.

Methyl- and vinyl-terminated self-assembled monolayers (SAM) on gold substrates were prepared by immersing the samples in a 1 mM solution of *n*-octadecanethiol (2 h) and undec-10-ene-1-thiol (12 h),

respectively, in ethanol. After removal from the thiol solution, the samples were rinsed with ethanol and dried with nitrogen.

Preparation of Silicon Substrates. Silicon (Si) substrates were cut from silicon wafers into 1.2 cm × 4 cm samples, sonicated in ethanol for 30 min, and dried in a stream of nitrogen. Then, the samples were exposed to piranha solution (14 mL of H_2SO_4/6 mL of H_2O_2) for 45 min to remove adventitious carbon and generate a hydroxylated surface. *Caution:* "Piranha" solution reacts violently with organic materials; it must be handled with extreme care. The samples were rinsed four times by submersion in water and once in ethanol and dried thoroughly in a stream of N_2.[15] Monolayers were formed on silicon surfaces by immersing the samples in a 1 mM solution of *n*-octadecyltrichlorosilane in anhydrous toluene for 5 h to obtain methyl-terminated monolayers. Upon removal from solution, the samples were rinsed in toluene and dried in a stream of N_2.

Preparation of Polyisoprene Substrates (PIP). Methyl-terminated monolayers on Si and Au were dip-coated in a 1 mM solution of *cis*-polyisoprene in hexane for 1 min after immersion at constant velocity of 18 mm/min using the precise displacement controller of a Sigma 70X 1000 IUP tensiometer by KSV Instruments Ltd. After the immersion time, the samples were withdrawn from the solution at a constant rate of 18 mm/min followed by drainage of the excess of polymer by immersion and withdrawing of the sample in pure hexane at a constant velocity of 45 mm/min. The excess of solvent was evaporated from the sample after exposure to laboratory conditions and before performing surface-initiated polymerization. Only one rinse was performed in this protocol as further rinses did not change the morphology of the film.

Preparation of Polymer Films. PIP films on Au or Si were placed under nitrogen in a septum-capped vial by 3 cycles of evacuation followed by N_2 backfilling. A 0.1 M solution of borane in THF was added to the vial via cannula. After 15 min of reaction, the borane solution was evacuated from the system and the samples were rinsed 3 times with anhydrous THF via cannula. To grow PM films from vinyl-terminated monolayers, a similar protocol was implemented. Finally, the samples were immersed in a 16 mM DM solution in diethyl ether at −17 °C for various times, and upon removal from the DM solution, they were vigorously rinsed with ethanol and dried in a stream of nitrogen. PM films were classified as SH if they exhibited advancing contact angle values[1] greater than 150° and hysteresis parameters ($H = \cos\theta_R - \cos\theta_A$)[16,17] lower than 0.14, as previously described by us.[18]

Oxidation of Hydroborated Films. In our experimental setup, hydroborated films could not be analyzed by infrared spectroscopy without becoming oxidized to varying degrees in transfer across the ambient air to the spectrometer. To aid in characterizing the hydroborated films on Au, we intentionally preoxidized[19] them by exposing freshly prepared films to O_2-saturated THF for 1 h and water for 30 min (HBO), followed by rinsing the monolayers with ethanol and water and drying them with a stream of nitrogen.

Characterization Methods. Thickness measurements of PM films were performed with a Veeco Dektak 150 profilometer for the case of the polymer films, using 49 μN of force and the hills and valleys detection mode. Thickness was estimated by scratching[13,20] the surface, scanning 500−1000 μm across the scratch and plane-fitting the scan results using the instrument software. In the case of thinner films (SAMs and PIP clusters), we used a J.A. Woollam XLS-100 variable angle spectroscopic ellipsometer. At a 75° angle of incidence, 100 revolutions/measurement were taken across a range of wavelengths (200−1000 nm) for each sample. WVASE 32 Version 3.374 software was used to model and calculate the thickness of the films. Fresh and uncoated Au substrates served as a baseline for thickness measurements and were used to determine the optical constants of the bare substrate. The film thickness was estimated as the average of three measurements at different points across the substrate, using the Cauchy model with the coefficients set at $A = 1.5$ and $B = C = 0$. Reported errors for both techniques represent the averages and standard deviations, respectively, from at least two independently prepared films.

Advancing and receding contact angles were measured with a Rame-Hart goniometer on static ~5 μL drops. A syringe was used to apply

an ethanol—water solution, in which the needle of the syringe remained inside the probe fluid droplet as the advancing and receding contact angle measurements were taken. Reported errors represent the averages and standard deviations, respectively, from at least four independently prepared films.

SEM images were obtained using a Raith e-Line electron beam lithography (EBL) system equipped with a thermal-assisted field emission gun at 10 keV. PM-IRRAS spectra were collected using a Bruker PMA-50 attachment to a Bruker Tensor 26 infrared spectrometer equipped with a liquid-nitrogen cooled mercury—cadmium—telluride (MCT) detector and a Hinds Instruments PEM-90 photoelastic modulator. The source beam used a half-wavelength ($\lambda/2$) retardation modulated at a frequency of 50 kHz and set at 80° incident to the sample surface. Spectra were collected over 5 min (380 scans) at a resolution of 4 cm^{-1}.

RESULTS AND DISCUSSION

Growth of SH Films from PIP Surfaces. Scheme 1 shows the process we designed to grow SH films from PIP clusters. First, olefin-rich PIP surfaces were prepared by dip-coating methyl-terminated films on silicon or gold into a 1 mM solution of PIP in hexane followed by rinsing in pure hexane.

Rinsing the PIP film produced small clusters that were firmly attached to the substrate (Figure 1b), as evidenced by the
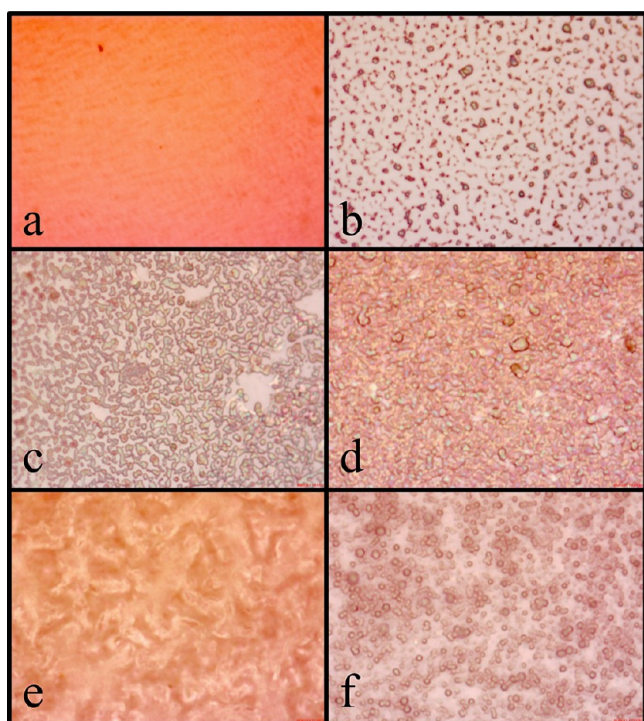

Figure 1. Optical images (100×) of (a) a methyl-terminated silicon surface, (b) a PIP surface and various PM/HB-PIP films after (c) 1 s, (d) 1 min, and (e) 10 min of polymerization, and (f) a SH PM film grown from a vinyl-terminated monolayer (PM/SAM) on gold after 24 h of polymerization.

observation that further extensive rinsing could not remove them. The reflectance IR spectrum of a PIP-modified gold surface (Figure 2) indicates much higher crystallinity than PIP exhibits in the liquid state,[21] as evidenced by asymmetric and symmetric methylene stretching modes at 2919 and 2851 cm^{-1}, respectively, rather than at 2926 and 2855 cm^{-1}, respectively, for the liquid film.[13] Additional characteristics that suggest differences in the packing and organization of the PIP chains
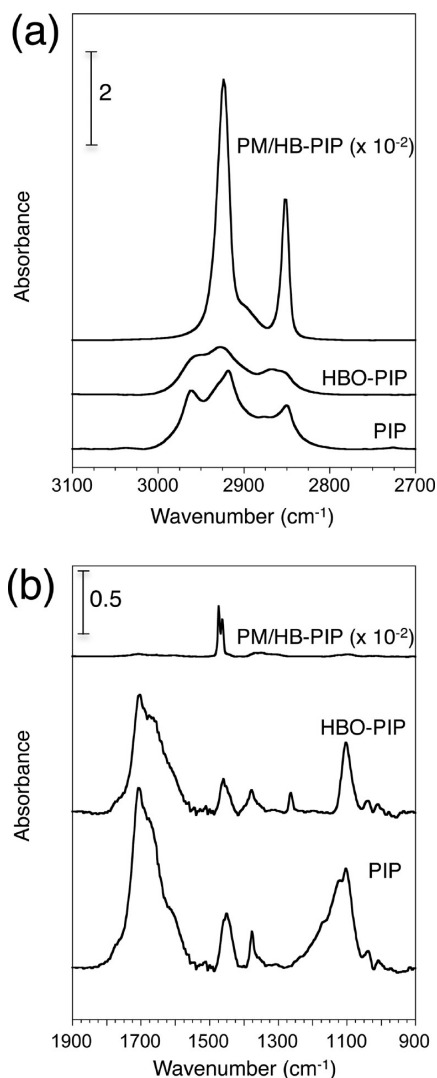

Figure 2. Reflectance-absorption IR characterization of the surface at different stages in the SIPM process. The listed films refer to a PIP surface on a methyl-terminated substrate (PIP), a hydroborated PIP film after going through a partial oxidation process (HBO-PIP), and a PM film grown from a hydroborated PIP substrate after SIPM (PM/HB-PIP). For proper comparison, the spectrum of the PM/HB-PIP film was multiplied by 0.01.

when confined at the surface is the shift in wavenumber of the CH$_3$ modes (ν_{as} = 2964 cm^{-1} → 2967 cm^{-1}, ν_s = 2880 cm^{-1} → 2876 cm^{-1}) from the liquid values and the appearance of the in-phase C=C stretching mode at 1700 cm^{-1}. Higher PIP crystallinity when coated onto a substrate is in agreement with the adhesive character of elastomers,[22] which provides the film with stability when exposed to various solvents.

To demonstrate the ability of these films to serve as substrates for the polymerization, we first hydroborated the internal olefins of the PIP films by exposure to BH$_3$. To verify that hydroboration took place, we subsequently oxidized the BH$_2$ moieties of the film by exposing them to an oxygen-saturated THF solution.[13,19] This exposure transforms the boranes into boronic acid groups that are more readily identified using IR spectroscopy (HBO-PIP). As a control, we also collected the IR spectrum for a PIP surface exposed to an oxygen-saturated THF solution, which did not exhibit signs of oxidation. IR results in Figure 2 show the appearance of a

mode at a 1263 cm^{-1} attributed to the symmetric B—O stretching,[23,24] indicating partial oxidation of the borane moieties. Presence of the C=C stretching vibration of the internal double bonds in the oxidized surface also indicates that the polymer chains were partially hydroborated and olefin groups are still available within the film. Hydroboration of PIP has been demonstrated by Minoura and Ikeda in solution-phase conditions.[25] However, their work reveals that the borane groups were partially oxidized to R—O—B groups as indicated by the 1340 cm^{-1} peak in their spectrum. Differences in nature of the oxidized borane species could be explained by different oxidation degrees due to the reorganization of the peroxide species initially formed upon oxidation.

Borane-modified PIP films were exposed to ether solutions of DM under inert atmosphere to grow PM films. Figure 1c–e shows optical images of the PM/HB-PIP surface after 1 s, 1 min, and 10 min of polymerization, and for comparison, Figure 1f shows a PM film grown from a vinyl-terminated SAM after 24 h of polymerization; shorter polymerizations yielded smoother surfaces for the SAM-initiated films. From Figure 1c, we observe that as soon as the activated surface is in contact with the DM solution, PM starts growing exclusively at the PIP microclusters distributed along the surface. This aspect is indicated by the decreased separation between the different polymer domains decorating the surface and the absence of growth at various regions along the surface that do not contain such domains. As the reaction proceeds and the domains grow, the PM film spreads along the surface and covers it almost completely after 1 min of reaction. At these conditions, PM clusters nucleate and form larger polymer aggregates along the surface. Finally, after 10 min of polymerization, the surface is completely covered, and the film is extremely rough compared to PM/SAM films (Figure 1f).

Figure 2 shows reflectance IR spectra of a PM/HB-PIP film after 1 min of polymerization; films prepared via longer polymerizations showed the same features with much greater intensities. From the IR spectrum, the PM/HB-PIP film exhibits CH$_2$ stretching and bending modes consistently found in linear PM,[26] thus indicating the successful polymethylenation of DM from the borane sites immobilized on the PIP surface. However, compared to the PM films grown from vinyl-terminated monolayers,[13] the crystallinity of PM/HB-PIP films is significantly lower as evidence by the shift of the CH$_2$ stretching modes toward higher values in wavelength (ν_{as} = 2924 cm^{-1}, ν_s = 2851 cm^{-1}). Lower crystallinity in these films could result from the geometric limitations that occur by having a much greater concentration of distinct growing PM chains that are initiated from the 3-D hydroborated PIP clusters, rather than having initiation spread over an entire 2-D surface.

Properties of the SH Films. Figure 3 compares the thickness behavior for the PM/HB-PIP and the PM/SAM films as a function of time. Experimental results in this figure indicate that both films exhibit a fast growth rate that slows as the reaction proceeds, suggesting increasing termination of active chains.[13] The macro-initiated film exhibits asymptotic thicknesses that are more than 4 times greater than the monolayer-initiated films. Fits of the data are based on a kinetic equation developed by Harada et al.[27] and later used by us[28] that assumes propagation to be dependent upon monomer and chain concentration and termination to be a first-order process with respect to active chain concentration,
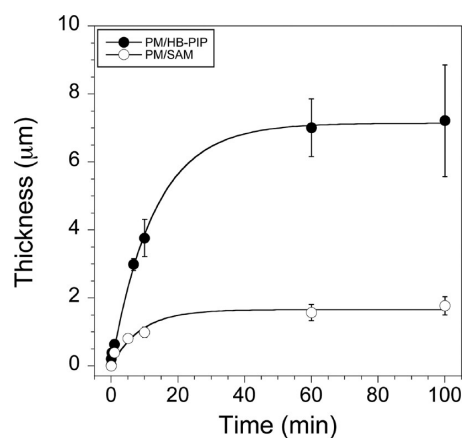

Figure 3. Time dependence of thickness for PM films grown from a PIP surface (PM/HB-PIP) and a vinyl-terminated monolayer (PM/SAM) using a 16 mM DM solution in ether at −17 °C.

$$d = \frac{KMm_o}{k_t\rho}(1 - e^{-k_t t})$$

$$(1)$$

where d is the film thickness at a given time, K is the propagation velocity that is a product of the propagation rate constant and the initial concentration of propagating chains, k_t is an apparent first-order termination rate constant, M is the monomer concentration (16 mol/m^3), m_o is the mass of the monomer unit (14 g/mol), and ρ is polymer density on the surface (estimated as 0.94 g/cm^3 for high density polyethylene). Results of the fits reveal that the propagation velocity is increased by a factor of 3 for the PIP-initiated PM film (3.9 × 10^{-5} m/s) over that for the SAM-initiated film (1.3 × 10^{-5} m/s), and its termination rate constant (0.0013 s^{-1}) is reduced by 30% from that of the SAM-initiated film (0.0019 s^{-1}). The combined greater propagation rate and lower termination rate indicate the high potential of these macro-initiated surfaces to rapidly grow thicker films when compared to surfaces that confine the active groups exclusively at the interface such as that of the SAMs. The higher propagation velocity for PM/HB-PIP films as compared to PM/SAM films is attributed to the greater number of borane sites that result from the internal olefin moieties distributed along every other carbon of the PIP chains when compared to a 2-D surface. We estimate that our HB-PIP film with an average thickness of 15 nm would have ~30 times more olefin moieties that could undergo hydroboration than a vinyl-terminated monolayer. In light of this factor of 30, the observed 3-fold increase in the propagation velocity suggests that 10% or fewer of these olefins are actually modified to yield active polymer chains or are accessible by the monomer for polymerization. In fact, many initiation sites would be buried deeply within the PIP cluster and may become rapidly occluded as the PM begins to grow. The lower termination rate for the HB-PIP film may be due to the fact that the actively propagating sites are initially distributed in 3-D space at and below the interface, rather than being confined at a 2-D surface and, thus, would be less accessible to terminating species.

We have also monitored water contact angle of the PM film as function of the polymerization time to establish the time scales at which superhydrophobicity can be achieved. Table 1 shows the dynamics of the advancing and the receding CAs as PM grows from HB-PIP films. To rationalize the CA behavior in Table 1, we first notice that only 1 s of polymerization is

Table 1. Advancing and Receding CA at Various Times in the SIPM Process from an HB/PIP Coating on Silicon[a]

time (s)	θ_a (°)	θ_r (°)
0	117 ± 4	54 ± 6
1	159 ± 1	91 ± 1
10	165 ± 2	98 ± 5
60	166 ± 1	156 ± 1
600	165 ± 1	160 ± 2
6000	165 ± 1	159 ± 2

[a]The 0 s data point represents a PIP surface.

sufficient to provide remarkable differences in wettability between the PM/HB-PIP and the PIP surfaces. Here, we also observe that the advancing CA is immediately boosted as the polymerization occurs and rapidly reaches a maximum value of 166° ± 1° within 1 min, while the receding angle climbs to 156 ± 1° within 1 min. This high advancing angle and low hysteresis indicate that the film becomes superhydrophobic within 1 min of polymerization. In contrast, a few days of film growth was required for PM films grown from vinyl-terminated monolayers on silicon to reach the state of superhydrophobicity, due to their smoother topography.[13] Here, longer polymerizations resulted in a decrease in hysteresis value below the 1 min value, consistent with a more stable super-hydrophobic state. Association of the CA behavior with the film thickness indicates that PM/HB-PIP films achieve SH behavior after 1 min of reaction and at a film thickness close to 600 nm.

The SH behavior of PM/HB-PIP results from the presence of topographic features able to entrap air at the polymer/water interface.[3,4] To more closely examine the morphology of the PM surfaces, we used SEM to obtain magnified images for the PM/HB-PIP (1 h) and the PM/SAM (24 h) films as shown in Figures 4a,b and 4c,d, respectively. Comparison of these images
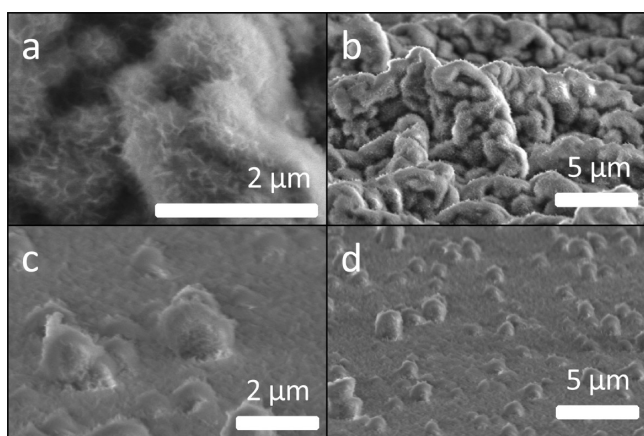

Figure 4. SEM images for PM films grown from (a, b) a PIP surface (PM/HB-PIP) and (c, d) a vinyl-terminated monolayer (PM/SAM).

confirms the remarkable differences in the shape and morphology of the microscale features present in both PM films. In the case of the features grown from SAMs, they consist of spheroids distributed randomly over the surface. However, in the case of films grown from PIP, the features cover the entire surface and the planar base of features is absent. These microscale features contain a rough, nanoscale hair-like outer topography (Figure 4a) that can be observed in as short as 1 s of polymerization as the microscale domains begin to merge

(Figure S1, Supporting Information). This hair-like nanoscale topography, combined with the microscale roughness produced by initiation of many PM chains within a single PIP cluster, produces the unique topography in this macro-initiated film and contributes toward the rapid attainment of super-hydrophobicity.

CONCLUSIONS

SH films made of the world's simplest polymer, PM, can be grown from hydroborated PIP surfaces in as little as 1 min of surface-initiated polymerization. The use of a macroinitiator here accelerates the rate of film growth by providing a greater concentration of active chains and thereby enhances the final film thickness well beyond that exhibited for PM grown by monolayer-based initiators. The PM film exhibits a rich and highly textured microscale topography consisting of partially fused PM clusters, as well as a rough, hair-like nanoscale topography. These results demonstrate the potential applicability of the fabrication technique described here to rapidly create robust and inexpensive SH coatings atop virtually any smooth substrate.

ASSOCIATED CONTENT

Ⓢ Supporting Information

An SEM image of merging PM clusters grown in only 1 s from an HB/PIP surface. This information is available free of charge via the Internet at http://pubs.acs.org/.

AUTHOR INFORMATION

Corresponding Author
*E-mail: kane.g.jennings@vanderbilt.edu.

Notes
The authors declare no competing financial interest.

ACKNOWLEDGMENTS

REFERENCES

(1) Dorrer, C.; Ruhe, J. *Soft Matter* **2009**, *5*, 51−61.
(2) Roach, P.; Shirtcliffe, N. J.; Newton, M. I. *Soft Matter* **2008**, *4*, 224−240.
(3) Doshi, D. A.; Shah, P. B.; Singh, S.; Branson, E. D.; Malanoski, A. P.; Watkins, E. B.; Majewski, J.; van Swol, F.; Brinker, C. J. *Langmuir* **2005**, *21*, 7805−7811.
(4) Asanuma, H.; Noguchi, H.; Uosaki, K.; Yu, H. Z. *J. Phys. Chem. C* **2009**, *113*, 21155−21161.
(5) McHale, G.; Newton, M. I.; Shirtcliffe, N. J. *Soft Matter* **2010**, *6*, 714−719.
(6) Mumm, F.; van Helvoort, A. T. J.; Sikorski, P. *ACS Nano* **2009**, *3*, 2647−2652.
(7) Persson, B. N. J.; Albohr, O.; Tartaglino, U.; Volokitin, A. I.; Tosatti, E. *J. Phys.: Condens. Matter* **2005**, *17*, R1−R62.
(8) de Leon, A. C.; Pernites, R. B.; Advincula, R. C. *ACS Appl. Mater. Interfaces* **2012**, *4*, 3169−3176.
(9) Saleema, N.; Sarkar, D. K.; Paynter, R. W.; Chen, X.-G. *ACS Appl. Mater. Interfaces* **2010**, *2*, 2500−2502.
(10) Zhu, X.; Zhang, Z.; Men, X.; Yang, J.; Xu, X. *ACS Appl. Mater. Interfaces* **2010**, *2*, 3636−3641.
(11) Hwang, H. S.; Kim, N. H.; Lee, S. G.; Lee, D. Y.; Cho, K.; Park, I. *ACS Appl. Mater. Interfaces* **2011**, *3*, 2179−2183.

(12) Lee, S. H.; Dilworth, Z. R.; Hsiao, E.; Barnette, A. L.; Marino, M.; Kim, J. H.; Kang, J.-G.; Jung, T.-H.; Kim, S. H. *ACS Appl. Mater. Interfaces* **2011**, *3*, 476−481.

(13) Tuberquia, J. C.; Nizamidin, N.; Harl, R. R.; Albert, J.; Hunter, J.; Rogers, B. R.; Jennings, G. K. *J. Am. Chem. Soc.* **2010**, *132*, 5725−5734.

(14) Black, H. *Aldrichimica Acta* **1983**, *16*, 3−10.

(15) Cione, A. M.; Mazyar, O. A.; Booth, B. D.; McCabe, C.; Jennings, G. K. *J. Phys. Chem. C* **2009**, *113*, 2384−2392.

(16) Chen, W.; Fadeev, A. Y.; Hsieh, M. C.; Oner, D.; Youngblood, J.; McCarthy, T. J. *Langmuir* **1999**, *15*, 3395−3399.

(17) Boulange-Petermann, L.; Gabet, C.; Baroux, B. *J. Adhes. Sci. Technol.* **2006**, *20*, 1463−1474.

(18) Tuberquia, J. C.; Nizamidin, N.; Jennings, G. K. *Langmuir* **2010**, *26*, 14039−14046.

(19) Brown, H. C.; Midland, M. M. *Tetrahedron* **1987**, *43*, 4059−4070.

(20) Manaka, T.; Ohta, H.; Iwamoto, M.; Fukuzawa, M. *Colloids Surf., A* **2005**, *257−258*, 287−290.

(21) Nallasamy, P.; Mohan, S. *Arabian J. Sci. Eng.* **2004**, *29*, 17−26.

(22) Sanchez-Adsuar, M. S. *Int. J. Adhes. Adhes.* **2000**, *20*, 291−298.

(23) Shurvell, H. F.; Faniran, J. A. *Can. J. Chem.* **1968**, *46*, 2082−2088.

(24) Faniran, J. A.; Shurvell, H. F. *Can. J. Chem.* **1968**, *46*, 2089−2095.

(25) Minoura, Y.; Ikeda, H. *J. Appl. Polym. Sci.* **1971**, *15*, 2219−2236.

(26) Bai, D.; Jennings, G. K. *J. Am. Chem. Soc.* **2005**, *127*, 3048−3056.

(27) Harada, Y.; Girolami, G.; Nuzzo, R. G. *Langmuir* **2003**, *19*, 5104−5114.

(28) Berron, B. J.; Graybill, E. P.; Jennings, G. K. *Langmuir* **2007**, *23*, 11651−11655.